Key Engineering Materials Vols. 413-414 (2009) pp 351-358
online at http://www.scientific.net

Bayesian Logic Applied to Damage Assessment of a Smart Precast Concrete Element

Daniele Zonta[1,a], Matteo Pozzi[1,b], Huayong Wu[1,c] and Daniele Inaudi[2,d]

[1] DIMS, University of Trento, Via Mesiano, 77, 38050 Trento, Italy

[2] SMARTEC SA, via Pobiette 11, CH-6928 Manno, Switzerland

[a]daniele.zonta@unitn.it, [b]matteo.pozzi@ing.unitn.it, [c]huayong.wu@ing.unitn.it, [d]inaudi@smartec.ch

Keywords: Bayesian analysis, Fiber optic sensors, SOFO, Smart structures, Precast concrete

Abstract. This paper presents the laboratory validation of a prototype optic-fiber instrumented structural element. The element is a reduced-scale reinforced concrete beam, of dimensions 3.8×0.3×0.5m that can be pre-stressed by an internal Dywidag bar. The sensing technology is based on a multiplexed version of the SOFO strain sensor, prepared in the form of a 3-field smart composite bar; in-line multiplexing is obtained by separating each measurement field through broadband FBGs. The experiment aims to identify the response of the sensors to differing damage conditions artificially produced in the element, including cracking and loss of prestressing. A numerical algorithm, based on Bayesian logic, is applied to real-time diagnosis: by processing the sensor measurements and prior information, the method assigns a posterior probability to each assumed damage scenario, as well as the updated probability distributions for each relevant structural parameter. With respect to classical damage detection approaches, the merit of those based on Bayesian logic is to provide not only information on the damage, but also the degree of confidence in this information. The paper discusses the ability of the system to identify the differing damage conditions. The reported test clearly shows that an occurrence such as a loss of prestressing can be recognized early with a high degree of reliability based on the strain data acquired.

Introduction

In the last decade, health monitoring and structural evaluation for bridges have attracted much attention. We cite for example the recent proceedings of IABMAS [1]. As the need for long term monitoring increases and new sensing technologies are developed, attempts are made to embed traditional or novel instruments into the structural elements, or even directly to integrate them with the materials used to build the structures. The concept of smart structure refers to systems able to provide information on their conditions and to adapt their behavior according to the current state, where the sensing technology is the first step to realize this idea. Most traditional condition monitoring devices, such as electrical strain gauges or piezoelectric accelerometers, are often not suited to use in a structural element as long-term sensing systems, because of their low durability. Conversely, fiber optic sensors (FOS), due to their small size, long transmission range with low loss and high immunity to corrosion and electro-magnetic interference, have come into wider use by the civil engineering community, especially for long term monitoring Udd [2], Ansari [3,4], Measures [5].

Recognizing the growing interest of the prefabrication industry in these technologies, the University of Trento has recently undertaken a research effort aimed at demonstrating the feasibility of precast smart element fabrication. A prototype of these elements, instrumented with fiber optics, has been produced and tested in the laboratory to assess its self-diagnosis capability. In the next section, we briefly introduce the reader to the prototype design and laboratory validation. In the following section, we formulate in detail the algorithm, based on Bayesian logic, applied to interpret measurement data: this methodology lets us identify not only the most likely values of the unknown damage parameters (such as type, position and extent) but also their posterior probability distribution. Then, we show how the system offers early recognition of different levels of prestress loss, artificially produced in the prototype during the experiment. The results are discussed at the end of the paper.

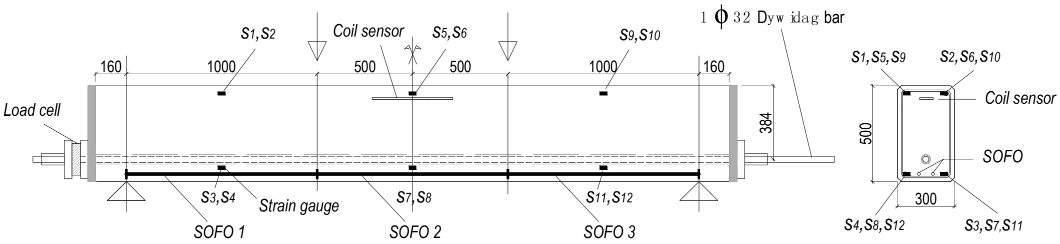

Fig.1 Side view and cross section of the prototype of smart element.

Prototype Design and Laboratory Test

The prototype, produced in view of the laboratory validation, is a reduced-scale prismatic reinforced concrete beam, of dimensions 3.8×0.3×0.5m (Fig. 1). Details of the beam design can be found in Zonta et al. [6]. The specimen reproduces in essence the main technological features of a full-scale prototype, which we expect to use in a new bridge. However, while in real-life precast elements are more likely to be produced using pre-tensioning technology, for this prototype we used a post-tensioning system, consisting of a Dywidag bar, because this lets us change the level of prestress during the experiment. The prototype was instrumented with a novel type of FOS, as well as traditional sensors, including 12 metal-foil strain gauges and 3 thermocouples. The FOS is a multiplexed version of the standard SOFO (Surveillance d'Ouvrages par Fibres Optiques) interferometric sensor, produced and commercialized by Smartec SA [7]. The multiplexed model, recently developed and tested by the authors [8], applies the same concept of the single SOFO to a discrete number of fields, separated, on the measurement and reference fibers, by Partial Reflectivity Mirrors (PRMs). The sensor scheme developed for this application includes 3 fields, 1.0 m long each, with a reference field 10 mm longer than the corresponding measurement base.

Following fabrication of the beam, a laboratory validation was carried out to correlate the response of the embedded sensor to different prestressing levels induced on the beam. The load protocol includes a sequence of load-unload cycles (labelled from T0 to T9), repeated under different values of pre-stressing and maximum vertical load, see Fig. 2 (a). A prestress load of 450 kN was calculated to produce a stress of 1 MPa in the concrete at the top edge of the unloaded beam. We calculated a nominal vertical load of 250 kN, to produce a stress of 2 MPa in the concrete at the lower edge of the fully prestressed beam. During the test, the prestress by the Dywidag bar was progressively reduced in each cycle to complete release, while the vertical load was released and reapplied to the nominal value in each cycle. Again, the reader is referred to Zonta et al. [6,9] for more details of the test procedures. Fig. 2(b) shows the time history recorded by SOFO, at the lateral and central segments of the beam, compared with those of two strain gages. The graph shows that the two types of the measurements are quite similar and allows recognition of the various load cycles, as well as the change in permanent deformation due to prestress release and creep, except SOFO1 in later stage, which may result from the non-uniform development of cracks along the

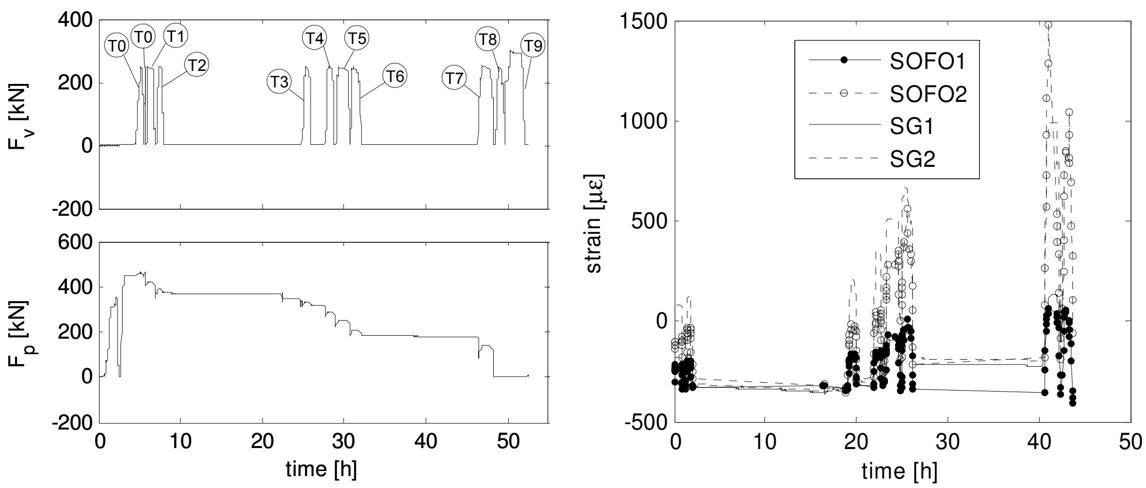

Fig. 2 (a) Load history applied to the element; (b) Time history recorded by SOFO system and strain gages (SG).

beam since the SOFO1 monitored the global deformation along the lateral field of beam.

Identification Concept

Compensated strain estimation. Once the monitoring data are available, a major issue is how to process the large amount of information acquired. For this application, a method based on Bayesian theory [10,11,12] has been developed to identify the different damage states of the pre-cast smart element through two steps corresponding to the two aspects of Bayesian theory: parameter estimation and model selection.

Assume we have a structure, instrumented with a certain number of sensors. Each sensor provides a measurement for each of Nt times ($t_1,t_2,\ldots,t_{Nt}$). It is convenient to divide them into two categories: *response sensors*, such as strain gauges, accelerometers, displacement transducers to record the structural responses of the bridge, and *environmental sensors*, such as thermocouples or load cells to record the load and environmental effects. To facilitate the effective use of a large amount of sensor measurements, here we divide the measurement components into two categories: one is an instantaneous term which changes frequently because of fluctuation of the external actions; the other results from the long term effect, constant in a certain period. In our case, Ns=15 strain sensors, including strain gauges and FOS, were installed working as the response sensors, labelled ($s_1,s_2,\ldots,s_{Ns}$); while Ne=4 environmental sensors were deployed and the load cell that records the vertical load is the only one used in the following analysis. Accordingly, it is convenient to organize measurements into time intervals, which are brief enough so that long term changes are negligible and long enough to ensure that short term changes are significant. Let us define the vector $\boldsymbol{\varepsilon}_{T,j}$ including all the strain measurements recorded by the sensor s_j within the time interval T and $\boldsymbol{\varepsilon}_T$ the matrix including all strains in time interval T. Finally let us label $\{\boldsymbol{\varepsilon}_T\}$ the whole dataset from the first time interval (i.e. from the start of monitoring) up to time T. Similarly, we define the matrix $\mathbf{h}_T$ as the external influences including all environmental measurements in time interval T. According to the design of the beam, if given the external loads, prestress level and taking the creep phenomenon into account, the strain measurements within time interval T can be expressed as follows:

$$\boldsymbol{\varepsilon}_T = \boldsymbol{\varepsilon}_T^V + \boldsymbol{\varepsilon}_T^P + \boldsymbol{\varepsilon}_T^{self} + \boldsymbol{\varepsilon}_T^{creep} + \boldsymbol{\varepsilon}_T^{noise} \tag{1}$$

where $\boldsymbol{\varepsilon}_T^V$ is the strain resulting from the external load and thermal effects, in our case basically the vertical load imposed by a hydraulic actuator; $\boldsymbol{\varepsilon}_T^P$ is the strain component related to the prestress levels; $\boldsymbol{\varepsilon}_T^{self}$ is the strain generated by the dead loads, here the weight of the concrete beam itself; $\boldsymbol{\varepsilon}_T^{creep}$ is the strain from the creep phenomenon; and $\boldsymbol{\varepsilon}_T^{noise}$ is the noise.

Then data acquired during this specific time interval (T) can be organized as the following matrix:

$$\boldsymbol{\varepsilon}_T = \boldsymbol{\varepsilon}_T^0 + \mathbf{h}_T \cdot \mathbf{a}_T + \mathbf{g}_T \tag{2}$$

where $\boldsymbol{\varepsilon}_T^0\,[N \times Ns]$ is strain independent of load or temperature (i.e. the compensated strain), corresponding to the term $\boldsymbol{\varepsilon}_T^0 = \boldsymbol{\varepsilon}_T^P + \boldsymbol{\varepsilon}_T^{self} + \boldsymbol{\varepsilon}_T^{creep}$, which is the long term component. $\mathbf{a}_T\,[Ne \times Ns]$ is the vector including the coefficients of the linear correlation from load to strain, which is supposed to be a constant in a specific time interval, together with the external load action, $\boldsymbol{\varepsilon}_T{}^V = \mathbf{h}_T \cdot \mathbf{a}_T\,[N \times Ns]$, to form the short term strain component. The noise is intended as the sum of two components: $\boldsymbol{\varepsilon}_T^{noise} = \mathbf{g}_T\,[N \times Ns] + e_T^{noise}\,[N \times Ns]$: $\mathbf{g}_T$ is the short-term noise matrix, related to measurement errors, which is assumed to have zero mean Gaussian distribution with standard deviation $(\sigma_g)_T$, while e_T^{noise} is a long term model error, supposed to be additive and normally distributed with zero mean value and standard deviation σ_T^m. Here N is the number of measurements recorded by a sensor during the time interval T.

According to the long term effect assumption, during a time interval the compensated strain for each sensor should stay constant, i.e. each value of any column in the matrix $\boldsymbol{\varepsilon}_T^0$ should be the same. If we consider the sensors one by one, the column vector of $\boldsymbol{\varepsilon}_T^0$ can be reduced to a single value in the time interval. Then Eq. 2 for sensor s_j can be rewritten as

$$\boldsymbol{\varepsilon}_{T,j} = \varepsilon_{T,j}^0 + \mathbf{h}_T \cdot \mathbf{a}_{T,j} + \mathbf{g}_{T,j} \tag{3}$$

As the long term strain component in time interval T can be represented by just one term $\varepsilon^0_{T,j}$, the processing of the measurements reduces to a linear equation with respect to the unknowns $\varepsilon^0_{T,j}$ and $\mathbf{a}_{T,j}$, recombined in matrix form as

$$[\boldsymbol{\varepsilon}_{T,j}]_{N\times 1} = \begin{bmatrix}\mathbf{h}_T & \mathbf{1}\end{bmatrix}_{N\times(Ne+1)} \cdot \begin{bmatrix}\mathbf{a}_{T,j} \\ \varepsilon^0_{T,j}\end{bmatrix}_{(Ne+1)\times 1} + [\mathbf{g}_{T,j}]_{N\times 1} \tag{4}$$

Here **1** is a column vector with N ones, and the subscript (e.g. $N\times 1$) gives the dimensions of the corresponding newly combined matrices. Now $[\mathbf{a}^T_{T,j}, \varepsilon^0_{T,j}]^T$ reduces to a new variable vector, and the whole problem becomes a parameter estimation: it is possible to formalize a rigorous Bayesian procedure to identify these quantities [6].

Scenario updating. Once the compensated strain is estimated, the method presented here allows for calculation of the probability of being in each scenario. If the probability during a time interval T-1 of being in a specific scenario is known, Bayes' theorem lets us update this probability using the fresh data acquired in time interval T. To apply the scenario updating procedure, 2 mutually exclusive and exhaustive scenarios have been assumed (S_1, S_2): S_1 denotes the state in which the beam suffers no loss at all, and S_2 is the state in which the beam suffers a certain percentage of prestress loss. Each scenario n is controlled by some random parameters $\boldsymbol{X}_n$, defined on a specific parameter domain $D\boldsymbol{X}_n$**.** According to the Bayesian theorem, the posterior probability of being in a scenario given the compensated strain can be expressed as

$$\text{prob}\left(S_n \left| \{\boldsymbol{\varepsilon}^0_T\}, I\right.\right) = \frac{\text{PDF}\left(\boldsymbol{\varepsilon}^0_T \left| \{\boldsymbol{\varepsilon}^0_{T-1}\}, S_n, I\right.\right) \cdot \text{prob}\left(S_n \left| \{\boldsymbol{\varepsilon}^0_{T-1}\}, I\right.\right)}{\text{PDF}\left(\boldsymbol{\varepsilon}^0_T \left| \{\boldsymbol{\varepsilon}^0_{T-1}\}, I\right.\right)} \tag{5}$$

where I indicates all the relevant background information [13].

The second term in the numerator of Eq. 5 is regarded as the *prior probability*, which represents our knowledge (or ignorance) as to the truth of the hypothesis before we have analysed the current data. Here we assume that the loss of the prestressing follows an increasingly monotonic change rule, i.e. it can not be recovered as the time interval goes on. During the updating process, we introduce a deterioration factor. We assume that the scenario prior information for the next interval depends only on the current step and has a probability p of staying in the undamaged state, and a probability of $1-p$ of going to the damaged state. That is, $P_{S_1\to S_1} = p$, and $P_{S_1\to S_2} = 1-p$, therefore it finally turns out to be a Markov process, of which the transition matrix is

$$P = \begin{bmatrix} p & 1-p \\ 0 & 1 \end{bmatrix} \tag{6}$$

Once we get the posterior probability of the ith step with respect to different scenarios, $P_i = [P_{i,1}, P_{i,2}]$, where $P_{i,1}, P_{i,2}$ are the probabilities of scenarios S_1, S_2 in the ith time interval respectively, we can update the prior information for the (i+1)th step as $\pi_{i+1} = P_i \times P$, where π_{i+1} denotes the updated prior information for the (i+1)th step. For the prior information in the first time interval, a uniform distribution of $[1/2, 1/2]$ was assigned, with the assumption of total ignorance at the beginning of the monitoring campaign. In this application $p = 8/9$ has been used to indicate a relatively slow evolution process from the conservative point of view.

The first term in the numerator of Eq. 5, sometimes referred to as *evidence* of scenario S_n, representing the probability of occurrence of the data if the specific scenario is given, can be calculated by integrating over the whole parameter domain $D\boldsymbol{X}_n$, using the marginalisation and product rule,

$$\text{PDF}\left(\varepsilon^0_T \left| \{\varepsilon^0_{T-1}\}, S_n, I\right.\right) = \int_{D\boldsymbol{X}_n} \text{PDF}\left(\varepsilon^0_T \left| \boldsymbol{X}_n, S_n, I\right.\right) \cdot \text{PDF}\left(\boldsymbol{X}_n \left| \{\varepsilon^0_{T-1}\}, S_n, I\right.\right) \cdot d\boldsymbol{X}_n \tag{7}$$

In scenario S_1, the beam is subject to no loss, the whole beam works in the elastic state, and the component of $\boldsymbol{\varepsilon}^P_T$ can be proved to be a constant; $\boldsymbol{\varepsilon}^{self}_T$ keeps constant and can be omitted automatically when removing the initial value of the time history. The creep term $\boldsymbol{\varepsilon}^{creep}_T$ is considered as stated in Eurocode 2 [13], due to the unknown prestressing level, and is supposed to follow the same value as estimated in the previous step when calculating the creep phenomena in the current time interval. If the smart element is estimated with more probability to be in scenario S_1, we consider the beam has suffered no loss and the full prestressing level is adopted in the calculation. Assuming that the noises from different sensors are independent of each other, then the likelihood function is just the product of the probabilities for the individual sensors. Based on the Gaussian noise assumption, one can directly calculate the likelihood of a given scenario S_1,

$$\mathrm{PDF}\left(\boldsymbol{\varepsilon}_T^0 \middle| \{\boldsymbol{\varepsilon}_{T-1}^0\}, S_1, I\right) \propto \exp(-\frac{1}{2}\chi^2) \tag{8}$$

where $\chi^2 = \sum(\varepsilon_{T,j}^r - \varepsilon_{T,j}^P)^2 / ((\sigma_{T,j}^0)^2 + (\sigma_{T,j}^{\mathrm{m}})^2)$, $\varepsilon_{T,j}^r = \varepsilon_{T,j}^0 - \varepsilon_{T,j}^{creep}$, of which j ranges from 1 to Ns, $\sigma_{T,j}^0$ is the standard deviation of the compensated strain, and $\sigma_{T,j}^{\mathrm{m}}$ the standard deviation of the model noise with a uniform distribution between 10 and $50\mu\varepsilon$.

In scenario S_2, the strain component $\boldsymbol{\varepsilon}_T^P$ is no longer modelled as constant, due to loss of prestressing level; if a prestressing loss percentage of α is assumed, we have $\boldsymbol{\varepsilon}_T^P = \{factor(\xi_k) \cdot F_{P,0} \cdot (1-\alpha)\}$. In order to account for the degradation of the concrete beam during loading, we introduced a distribution factor to determine the stiffness between the undegraded and fully cracked conditions [14]. $factor(\xi_k)$ is a nonlinear function of the concrete stiffness,

$$factor(\xi_k) = \pm(k_1(1-\xi_k) + k_2\xi_k)/(E_c I_0(1-\xi_k) + E_c I_c \xi_k) + 1/(E_c A_0(1-\xi_k) + E_c A_c \xi_k) \tag{9}$$

where k_1, k_2 are two constants, I_0, A_0 and I_c, A_c are moments of inertia and cross section areas in the initial and fully cracked conditions. E_c is Young's modulus. In this case two parameters, ξ_1 and ξ_2, have been introduced, corresponding to the two distribution factors in the lateral and middle sections respectively, $F_{P,0}$ denotes the full prestressing level, E_c=24*Mpa* was used from the sample tests. Hence in scenario S_2 the parameter vector can be specified as $\boldsymbol{X}_2 = \{\alpha, \xi_1, \xi_2\}$, Eq. 7 becomes:

$$\mathrm{PDF}\left(\boldsymbol{\varepsilon}_T^0 \middle| \{\boldsymbol{\varepsilon}_{T-1}^0\}, S_2, I\right) = \int \mathrm{PDF}\left(\boldsymbol{\varepsilon}_T^0 \middle| \boldsymbol{X}_2, S_2, I\right) \cdot \mathrm{PDF}\left(\boldsymbol{X}_2 \middle| \{\boldsymbol{\varepsilon}_{T-1}^0\}, S_2, I\right) \cdot d\boldsymbol{X}_2 \tag{10}$$

According to the Gaussian noise assumption, the first term of the integration can be calculated as

$$\mathrm{PDF}\left(\boldsymbol{\varepsilon}_T^0 \middle| \boldsymbol{X}_2, S_2, I\right) \propto \exp(-\frac{1}{2} \cdot \chi^2) \tag{11}$$

where χ^2 follows the same form as above, but with 3 parameters. For the prior assignment of the parameters in Eq. 10, in keeping with our ignorance before analysis of the current data, we take a simple uniform PDF for the first time interval as follows, $0 \le \alpha \le 1$, $0 \le \xi_1 \le 1$, $0 \le \xi_2 \le 1$. Then the corresponding prior information can be given:

$$\mathrm{PDF}\left(\boldsymbol{X}_2 \middle| \{\boldsymbol{\varepsilon}_{T-1}^0\}, S_2, I\right) = \frac{1}{(1-0)^3} \tag{12}$$

In order to calculate the likelihood in Eq. 10, suppose there are a set of 3 parameters $\boldsymbol{X}_0 = \{\alpha, \xi_1, \xi_2\}$, which yield the best fit to the data $\chi^2_{\min}$, taking a quadratic Taylor series expansion about this point,

$$\chi^2 = \chi^2_{\min} + \frac{1}{2}(\boldsymbol{X}_2 - \boldsymbol{X}_0)^T \nabla\nabla\chi^2(\boldsymbol{X}_0)(\boldsymbol{X}_2 - \boldsymbol{X}_0) \tag{13}$$

Since $\boldsymbol{X}_0$ is the best estimate fitting to the $\chi^2_{\min}$, the first derivative term should be zero, while terms with higher order than 3 are rejected. Replacing χ^2 of Eq. 11 with Eq. 13, substituting both Eqs. 11 and 12 into Eq. 10, except for the constant term, the integral of the related 3-dimensional multivariate Gaussian can be calculated,

$$\iiint \exp(-\frac{1}{4}(\boldsymbol{X}_2 - \boldsymbol{X}_0)^T \nabla\nabla\chi^2(\boldsymbol{X}_0)(\boldsymbol{X}_2 - \boldsymbol{X}_0)) d\alpha d\xi_1 d\xi_2 = \frac{(4\pi)^{3/2}}{\sqrt{\det(\nabla\nabla\chi^2(\boldsymbol{X}_0))}} \tag{14}$$

where $\det(\nabla\nabla\chi^2(\boldsymbol{X}_0))$ is the determinant of the Hessian matrix.

In order to find the parameter set $\{\alpha, \xi_1, \xi_2\}$ to yield the best fit of $\chi^2_{\min}$, we first divide the two nonlinear parameters ξ_1 and ξ_2 into 5 discrete points within the range $0 \le \xi_1 \le 1$, $0 \le \xi_2 \le 1$. For each of these discrete combinations of ξ_1 and ξ_2, a best estimate of α, labelled as μ_α, can be easily obtained, since it is a linear factor over the range, to optimize the minimum of $\chi^2_{\min}$. After a search of all the combinations of ξ_1, ξ_2 and α, an 'initial good set' of $\{\alpha, \xi_1, \xi_2\}$ to fit to the approximate $\chi^2_{\min}$ can be found. For a second step, the sequential simplex algorithm [14] has been used to find a more precise estimate of $\boldsymbol{X}_0$ based on the above 'initial good set', and it can be further refined with Newton-Raphson algorithm for the final step. On the basis of the Hessian matrix evaluated at $\boldsymbol{X}_0$, the covariance matrix σ^2 of the estimated parameter set can also be characterized. This is inversely related to the quadratic part of Eq. 13, $\sigma^2 = 2\cdot(\nabla\nabla\chi^2(\boldsymbol{X}_0))^{-1}$; therefore, the variance of estimated μ_α is $\sigma^2_\alpha = [2\cdot(\nabla\nabla\chi^2(\boldsymbol{X}_0))^{-1}]_{11}$, and the estimated α in the time interval T could be expressed as the normal distribution of $\alpha_T \sim N(\mu_{\alpha,T}, \sigma^2_{\alpha,T})$.

The identification for the first time interval relies only on prior information, but afterwards the prior assignment of parameters in Eq. 10 can be updated based on the already estimated parameter $\boldsymbol{X}_0$ in the previous step. If we assume that the loss of prestressing is constant along successive intervals, the posterior distribution obtained in the previous step can be directly employed as a new prior distribution. However we adopt a more realistic model according to which the prestressing loss parameter α can monotonically increase with time. To include this assumption in the updating process we built the prior knowledge for step T+1 by adding $\Delta\alpha$, a normally distributed parameter of variation for prestressing, to the posterior pdf of α in step T. The distribution of $\Delta\alpha$ is supposed to be $N(\mu_{\Delta\alpha}, \sigma^2_{\Delta\alpha})$. In our case $\Delta\alpha \sim N(0.1, 0.04)$ could be employed. Thus, from the second time interval on, the prior information of parameter, α, can be updated as

$$\pi_{\alpha,T+1} \sim N(\mu_{\pi,T+1}, \sigma^2_{\pi,T+1}) \tag{15}$$

where $\mu_{\pi,T+1} = \mu_{\alpha,T} + \mu_{\Delta\alpha}$, $\sigma^2_{\pi,T+1} = \sigma^2_{\alpha,T} + \sigma^2_{\Delta\alpha}$. $\pi_{\alpha,T+1}$ denotes the updated prior information of α for the (T+1) step.

Besides α, the other two parameters ξ_1 and ξ_2, are still treated as uniform distributions due to their random variation among different time intervals, i.e. $0 \le \xi_1 \le 1$, $0 \le \xi_2 \le 1$.

Then the prior assignment in Eq. 10 finally becomes,

$$\mathrm{PDF}\left(\boldsymbol{X}_2 \middle| \{\varepsilon^0_{T-1}\}, S_2, I\right) = \frac{1}{\sqrt{2\pi}\sigma_{\pi,T}} \cdot \frac{1}{(1-0)^2} \cdot \exp\left(-\frac{(\alpha-\mu_{\pi,T})^2}{2\sigma^2_{\pi,T}}\right) \tag{16}$$

Substituting Eqs. 11 and 16 into Eq. 10,

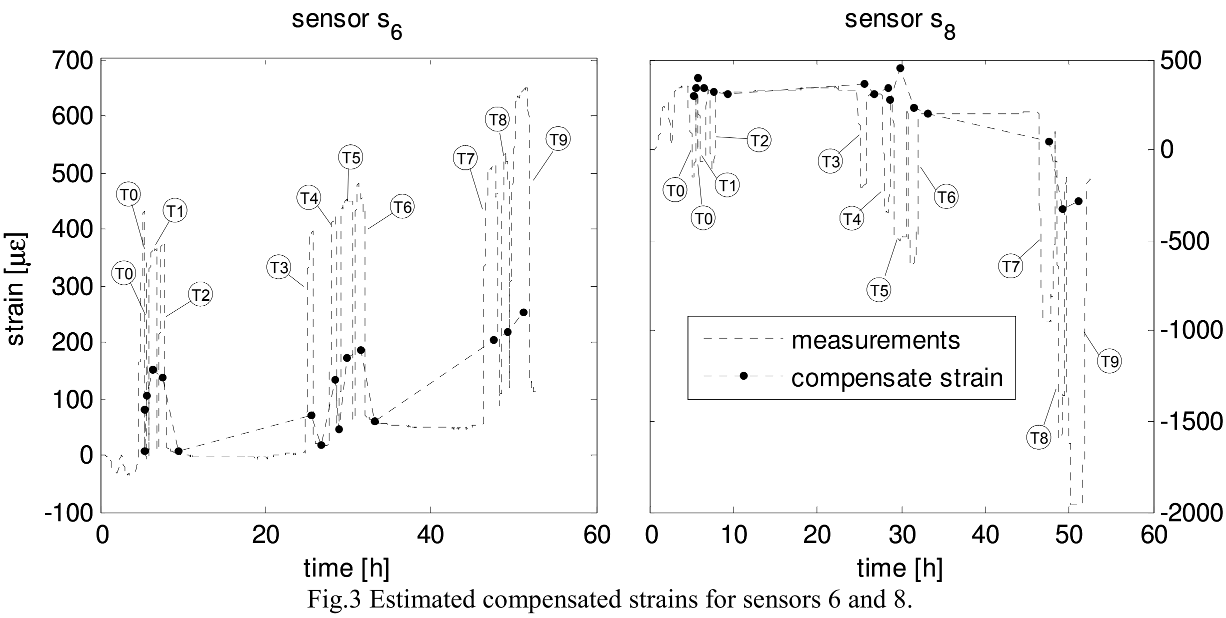

Fig.3 Estimated compensated strains for sensors 6 and 8.

$$\mathrm{PDF}\left(\varepsilon_T^0 \left| \{\varepsilon_{T-1}^0\}, S_2, I\right.\right) \propto \int \exp(-\frac{1}{2}\chi^2)\cdot\frac{1}{\sqrt{2\pi}\sigma_{\pi,T}}\cdot\frac{1}{(1-0)^2}\cdot\exp(-\frac{(\alpha-\mu_{\pi,T})^2}{2\sigma_{\pi,T}^2})\cdot d\boldsymbol{X}_2 \propto$$
$$\propto \frac{1}{\sqrt{2\pi}\sigma_{\pi,T}}\cdot\int \exp[-\frac{1}{2}(\chi^2+\frac{(\alpha-\mu_{\pi,T})^2}{2\sigma_{\pi,T}^2})]\cdot d\boldsymbol{X}_2 \propto \frac{1}{\sqrt{2\pi}\sigma_{\pi,T}}\cdot\int \exp(-\frac{1}{2}\cdot\hat{\chi}^2)\cdot d\boldsymbol{X}_2 \qquad (17)$$

where $\hat{\chi}^2 = \chi^2 + (\alpha-\mu_{\pi,T})^2/(2\sigma_{\pi,T}^2)$, the integration in Eq. 17 could be calculated in the same way as in Eqs. 13 and 14.

Application to the Smart Element

In our case, the loss of prestress was identified and can be compared with the actual preload recorded by the load cell applied to the Dywidag bar. In order to apply the procedure, the whole time history is divided into 16 time intervals, each interval including either a complete loading sequence or a period with no vertical load applied. According to the method presented in section *Compensated strain estimation*, the compensated strains were calculated to remove the vertical load dependent strains for each sensor. Fig. 3 shows the estimated results for the sensors 6 and 8.

Then based on the estimated compensated strain, we estimated the posterior distribution of different scenarios according to the procedure introduced in section *Scenario updating*. In the meantime, the reliability of the estimated prestress loss in each time interval was also studied.

Fig. 4 (top) indicates the probability distribution of scenario S_2 along the different time intervals. For the first 3 time intervals, S_1 dominates the identification process, which means the beam is supposed to be subject to no prestress loss. From the 4th time interval, the probability fluctuates between S_1 and S_2, and gradually S_2 become more probable. It seems the beam will suffer some loss, but the model cannot give us an estimate. As from the 7th interval, S_2 dominates; that is to say, from this stage the pre-load is suffering a loss. If we consider the mean value of the normal distribution as the best estimate of the corresponding prestress loss, the comparison between estimated and tested loss in Fig. 4 (bottom) shows that the tested results more or less lie in the zone of the mean value plus or minus the standard deviation. The curves in the figure give the estimated distribution of prestress loss with respect to different intervals. We can see that the proposed method is capable of tracking the various damage states of the beam.

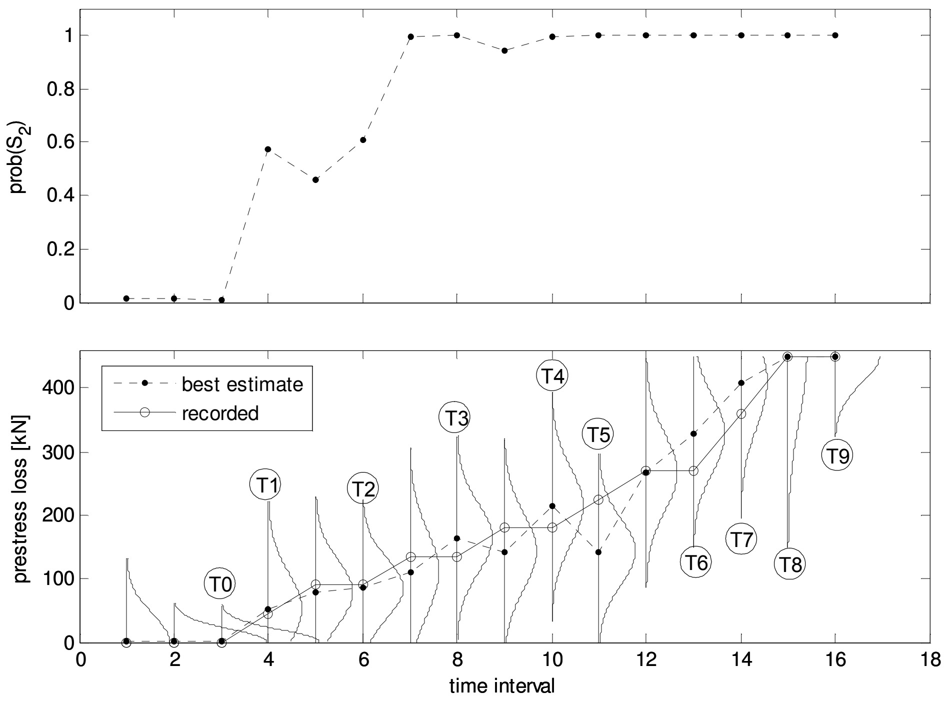

Fig. 4 Probability of scenario S_2 at different time intervals (top); comparison between the estimated prestress loss and that recorded at the load cell (bottom).

Summary

A smart element carrying a fiber optic sensing system was designed and tested in the laboratory under various damage situations. The data acquired during the experiment shows that the response performance of the optical system is more than satisfactory, especially when compared to traditional electrical sensors.

The proposed Bayesian identification procedure provides a rational quantification of the influence of monitoring data on knowledge of the occurrence of differing damage scenarios. With respect to classical damage detection methods, its merit is to provide not only information on the damage, but also the degree of confidence in this information. This is of paramount importance when the results of damage assessment serve as input in decision-making processes. The application of this procedure to the condition assessment of the smart element prototype highlights the possibilities of this approach. For example the reported test clearly shows that an occurrence such as a loss of prestress can be recognized early with a high degree of reliability based on the strain data acquired. It is interesting to observe that the probability of this damage scenario becomes immediately very high, independently of the precision of the damage parameters identified.

Despite the fact that the example provided is very specific, the approach presented here is not problem dependent, which can be able to process rationally all the available prior information, as well as model or material uncertainties , and could be further extended to manifold scenarios.

Acknowledgements

This work was funded by the Italian Earthquake Engineering Laboratory Network (ReLUIS) within the scope of the DPC-ReLUIS 2005-2008 project, Research Line n.10 "Definizione e sviluppo di archivi di dati per la valutazione del rischio, la pianificazione e la gestione dell'emergenza". The multiplexed SOFO sensor presented was deployed at the University of Trento in cooperation with Smartec SA: the effort of the whole Smartec production team is acknowledged. Finally, the authors wish to thank Matteo Faccincani, Alessandro Lanaro and Manuel Massella for their collaboration in developing and testing the smart element prototype.

References

[1] H.M. Koh, and D.M. Frangopol (Eds.): *Bridge Maintenance, Safety, Management, Health Monitoring and Informatics* (Balkema, Rotterdam 2008).

[2] E. Udd (Ed.): Fiber Optic Sensors: An Introduction for Engineers and Scientists (Wiley-Interscience, Hoboken 1991).

[3] F. Ansari (Ed.): Fiber Optic Sensors for Construction Materials and Bridges (Technomic Publishing Co, Lancaster 1998).

[4] F. Ansari, in: Proc. of the US - Europe Workshop on Sensors and Smart Structures Technology, Wiley (2003).

[5] R.M. Measures: Structural monitoring with fiber optic technology (Academic Press, London 2001).

[6] D. Zonta, M. Pozzi, H.Y. Wu, and D. Inaudi, in: Sensors and smart structures technologies for civil, mechanical, and aerospace systems 2008, Proc. of the SPIE, Vol. 6932 (2008).

[7] Information on http://www.smartec.ch/

[8] M. Pozzi, D. Zonta, H.Y. Wu, and D. Inaudi: Optical Fiber Technology Vol. 14 (2008), p. 281

[9] D. Zonta, M. Pozzi, H.Y. Wu, and D. Inaudi, in: Proc. 4th European Workshop on Structural Health Monitoring, DEStech Publications (2008).

[10] T. Bayes: Philosophical Transactions of the Royal Society of London, Vol. 53 (1763), p. 370

[11] P. Gregory: Bayesian Logical Data Analysis for the Physical Sciences (Cambridge University Press, Cambridge 2005).

[12] D.S. Sivia: Data Analysis: a Bayesian Tutorial (Oxford University Press, Oxford 1996).

[13] European Committee for Standardisation (CEN): EN 1992-1-1. Eurocode 2: Design of Concrete Structures – Part 1-1: General Rules and Rules for Buildings (CEN, Bruxelles 2004).

[14] F.H. Walters, J.L.R. Parker, S.L. Morgan, S.N. Deming: Sequential Simplex Optimization (CRC Press, Boca Raton 1991).

Damage Assessment of Structures VIII
doi:10.4028/www.scientific.net/KEM.413-414

Bayesian Logic Applied to Damage Assessment of a Smart Precast Concrete Element
doi:10.4028/www.scientific.net/KEM.413-414.351

References

[1] H.M. Koh, and D.M. Frangopol (Eds.): Bridge Maintenance, Safety, Management, Health Monitoring and Informatics (Balkema, Rotterdam 2008).

[2] E. Udd (Ed.): Fiber Optic Sensors: An Introduction for Engineers and Scientists (Wiley-Interscience, Hoboken 1991).

[3] F. Ansari (Ed.): Fiber Optic Sensors for Construction Materials and Bridges (Technomic Pub-lishing Co, Lancaster 1998).

[4] F. Ansari, in: Proc. of the US - Europe Workshop on Sensors and Smart Structures Technol-ogy, Wiley (2003).

[5] R.M. Measures: Structural monitoring with fiber optic technology (Academic Press, London 2001).

[6] D. Zonta, M. Pozzi, H.Y. Wu, and D. Inaudi, in: Sensors and smart structures technologies for civil, mechanical, and aerospace systems 2008, Proc. of the SPIE, Vol. 6932 (2008).

[7] Information on http://www.smartec.ch/

[8] M. Pozzi, D. Zonta, H.Y. Wu, and D. Inaudi: Optical Fiber Technology Vol. 14 (2008), p. 281
doi:10.1016/j.yofte.2008.01.006

[9] D. Zonta, M. Pozzi, H.Y. Wu, and D. Inaudi, in: Proc. 4th European Workshop on Structural Health Monitoring, DEStech Publications (2008).

[10] T. Bayes: Philosophical Transactions of the Royal Society of London, Vol. 53 (1763), p. 370
doi:10.1098/rstl.1763.0053

[11] P. Gregory: Bayesian Logical Data Analysis for the Physical Sciences (Cambridge University Press, Cambridge 2005).

[12] D.S. Sivia: Data Analysis: a Bayesian Tutorial (Oxford University Press, Oxford 1996).

[13] European Committee for Standardisation (CEN): EN 1992-1-1. Eurocode 2: Design of

Con-crete Structures – Part 1-1: General Rules and Rules for Buildings (CEN, Bruxelles 2004).

[14] F.H. Walters, J.L.R. Parker, S.L. Morgan, S.N. Deming: Sequential Simplex Optimization (CRC Press, Boca Raton 1991).